



Interaction between BaCO_3 and OPC/BFS composite cements at 20 °C and 60 °C

C.A. Utton^{a,*}, E. Gallucci^b, J. Hill^c, N.B. Milestone^a

^a University of Sheffield, Immobilisation Science Laboratory, Department of Materials Science and Engineering, Mappin Street, Sheffield S1 3JD, UK

^b Ecole Polytechnique Federale de Lausanne, Laboratory of Construction Materials, CH-1015 Lausanne, Switzerland

^c AMEC NNC Ltd, Birchwood, Cheshire, WA3 6GN, UK

ARTICLE INFO

Article history:

Received 5 November 2010

Accepted 11 November 2010

Keywords:

Radioactive waste
Waste management
Blended cement
 BaCO_3

ABSTRACT

A BaCO_3 slurry, containing radioactive ^{14}C , is produced during the reprocessing of spent nuclear fuel. This slurry is encapsulated in a Portland-blastfurnace slag composite cement. The effect of BaCO_3 on the hydration of OPC and Portland-blastfurnace slag cements has been studied in this work. Samples containing a simulant BaCO_3 slurry were cured for up to 720 days at 20 and 60 °C and analysed by XRD, SEM(EDX) and ICC. BaCO_3 reacted with OPC to precipitate BaSO_4 from a reaction between soluble sulfate and BaCO_3 . Calcium monocarboaluminate subsequently formed from the carbonate released. The monocarboaluminate precipitated as crystals in voids formed during hydration. At 60 °C in OPC, it was not identified by XRD, suggesting the phase is unstable in this system around this temperature. In the Portland-blastfurnace slag cements containing BaCO_3 , less monocarboaluminate and BaSO_4 were formed, but the hydration of BFS was promoted and monocarboaluminate was stable up to 60 °C.

© 2010 Elsevier Ltd. All rights reserved.

1. Introduction

A radioactive ^{14}C containing slurry of BaCO_3 , is produced from nuclear fuel reprocessing at the Thermal Oxide Reprocessing Plant (THORP) at Sellafield, UK. This slurry is classified as an intermediate level waste (ILW), and is typically encapsulated in a 9:1 blast furnace slag: Ordinary Portland cement (BFS:OPC) blended system. To fully understand the interactions within this ternary composite cement, the interactions between this system, neat OPC and BaCO_3 were studied.

^{14}C is an important radioactive element to consider in a waste stream, as it has a long half life (5730 years) and will actively combine with other elements within its environment replacing stable $^{12,13}\text{C}$ [1], making the species mobile, and a challenge to immobilise. Gases released during the THORP process, where spent uranium oxide fuel is dissolved in nitric acid, include $^{14}\text{CO}_2$ and ^{14}CO . These gases are passed through a caustic scrubber to remove any $^{14}\text{CO}_2$ and ^{14}CO forming sodium carbonate. The resulting solution is treated with $\text{Ba}(\text{NO}_3)_2$, precipitating $\text{Ba}^{14}\text{CO}_3$, which is allowed to settle, forming a waste slurry which is dewatered to give a final waste stream containing 20–30 wt.% $\text{Ba}^{14}\text{CO}_3$ precipitate in a solution of 10 wt.% soluble salts [2].

Literature published on the interactions between OPC based systems and BaCO_3 is limited, but there is extensive literature on the reactions between calcium carbonate (CaCO_3) and OPC, where CaCO_3 is used as a filler material [3–9]. Filler materials are inert or mildly reactive materials which replace a proportion of the cement to reduce costs and improve

physical properties [10]. CaCO_3 is often used in the construction industry with up to 5% limestone filler incorporated in Portland cement without formally declaring its presence [11]. Limestone is often used as an aggregate in concrete, but normally only the very fine material reacts. Studies of CaCO_3 additions are useful when comparing the addition of BaCO_3 .

Barium is in Group II of the periodic table, below calcium and strontium and is the largest and most electropositive, which influences its substitution reactions. The difference in solubility between the carbonates, hydroxides and sulfates of the Group II elements (Table 1) will affect reactions. It is interesting to note that barium sulfate is less soluble than barium carbonate, whereas all forms of calcium sulfate are more soluble than calcium carbonate. Both calcium and strontium readily form or substitute into Aft/AFm type phases. However barium, being a much larger cation, is reported to not form a fully substituted Aft phase [12]. Dumitru et al. [13,14] also reported only partial substitution of barium into an AFm calcium monocarboaluminate phase, using EDX analysis. The CO_3^{2-} ion once released into the solution is expected to react in the same manner, within the cement environment, regardless of its source.

The addition of CaCO_3 to OPC changes both the hydration products formed and the rate of the hydration reactions. In OPC hydrated with CaCO_3 , an AFm phase, calcium monocarboaluminate, $\text{Ca}_4\text{Al}_2(\text{CO}_3)(\text{OH})_{12} \cdot 5\text{H}_2\text{O}$ (Mc), forms through a reaction between C_3A and CaCO_3 [3,10]. Monocarboaluminate forms instead of monosulfate, which has the effect of stabilising ettringite (Al/S ratio stays high). It is also reported that a hemicarboaluminate phase, $(\text{Ca}_4\text{Al}_2(\text{CO}_3)_{0.5}(\text{OH})_{13} \cdot 5.5\text{H}_2\text{O})$, precedes the formation of Mc, where the activity of the carbonate is low [7,9,16].

* Corresponding author.

E-mail address: c.utton@sheffield.ac.uk (C.A. Utton).

Table 1
Solubility of selected calcium, strontium and barium compounds at 20–25 °C [15].

Chemical	Solubility ^(temp. °C) g/100 cc H ₂ O
Ca(OH) ₂	0.160 ²⁰
CaCO ₃	0.00066 ²⁰
CaSO ₄ ·2H ₂ O	0.205 ²⁰
Sr(OH) ₂	2.25 ²⁵
SrCO ₃	0.00034 ²⁰
SrSO ₄	0.0135 ²⁵
Ba(OH) ₂ ·8H ₂ O	4.91 ²⁵
BaCO ₃	0.0014 ²⁰
BaSO ₄	0.00031 ²⁰

Mc is an AFm phase, analogous to monosulfate, where SO₄^{2−} ions are replaced by CO₃^{2−} ions [10]. Although there is an equivalent carbonate phase to ettringite with the general formula Ca₆Al₂(SO₄)₃(OH)₁₂·26H₂O, known as calcium tricarboaluminate, this phase does not form in cements with carbonate additions as, of the two carbonate AFt/AFm phases, Mc is the more stable phase with a greater insolubility at ambient temperatures [3,17].

Typically only a maximum of 2–3 wt.% CaCO₃ reacts with OPC at ambient temperatures [10]. Additions of less than 5 wt.% CaCO₃ have been found to accelerate initial hydration and decrease porosity [7] as well as increasing early strength [18,19]. Higher additions of greater than 10–15 wt.% were found to increase porosity and decrease the compressive strength [8].

Limited studies on the addition of barium carbonate, or soluble barium salts to OPC have been reported. The reaction of BaCO₃ with C₃A and OPC is similar to that of CaCO₃. Dumitru et al. [13,14] reported that BaCO₃ delays the hydration of C₃A, forming a hemicarboaluminate phase containing 6 wt.% of barium (determined by EDX). Reacting OPC and BaCO₃ resulted in the formation of monocarboaluminate and large quantities of BaSO₄, from the reaction between gypsum and BaCO₃. Ettringite formation was also suppressed, with setting times prolonged, in proportion to the amount of BaCO₃ added. The addition of barium as a soluble salt, such as barium nitrate, also resulted in the precipitation of BaSO₄ and BaCO₃ [20]. It was suggested that the presence of large quantities of insoluble compounds hinders OPC hydration resulting in lower non-evaporable water contents and a greater proportion of anhydrous OPC [21].

In practice, the radioactive waste Ba¹⁴CO₃ slurry is mixed with a BFS:OPC composite cement, forming a complex ternary system. Mendéndez et al. [22] reported the strength development of a ternary blended cement system containing OPC, between 0% and 35% BFS and between 0% and 15% CaCO₃. CaCO₃ improved the early strength while BFS improved later strength and refined the pore system. The ternary systems therefore offered an improvement in strength properties over binary cements of either combination. But, a limit exists as adding vast quantities of filler material will negate these effects, decreasing the overall strength due to cement dilution [2].

In this paper the effect of a simulated ¹⁴C containing waste slurry, in the form of BaCO₃ dispersed in distilled water, on the hydration of OPC and a 9:1 BFS:OPC composite cement, is presented, alongside a simplified system containing C₃A, CaSO₄·2H₂O and BaCO₃.

2. Materials and experimental procedure

2.1. Raw materials

OPC (Castle Cements) used had a fineness of 352 m²/kg Blaine. The BFS (Redcar steel works) was a coarsely ground granulated blast furnace slag, with a fineness of 286 m²/kg Blaine. Oxide compositions of these materials are presented in Table 2. A coarse ground BFS is used for waste encapsulation to minimise heat of hydration, which

Table 2
Chemical analysis (XRF) of OPC and BFS.

Chemical analysis	OPC, wt.%	BFS, wt.%
CaO	64.58	42.1
SiO ₂	20.96	34.5
Al ₂ O ₃	5.24	13.74
Fe ₂ O ₃	2.61	0.97
MgO	2.09	7.29
SO ₃	2.46	–
K ₂ O	0.59	0.49
Na ₂ O	0.28	0.22
Chloride	0.048	0.022
Insolubles	0.27	–
Loss on ignition	0.73	–1.05

may result in thermal cracking. A simulated waste slurry was prepared by mixing analytical grade BaCO₃ (Sigma Aldrich) with distilled water, in a high shear mixer. Although the actual waste produced at THORP also contains soluble salts in the solution, these compounds were omitted to simplify the system and purely assess the effect of BaCO₃ alone on hydration. It is understood that the presence of soluble salts could effect hydration, with likely acceleration of reactions.

2.2. Sample preparation

Neat OPC and 9:1 BFS:OPC systems were mixed in a Hobart mixer with a water to solid ratio (w/s) of 0.37 and cured at 20 °C and 60 °C at 95% RH for up to 720 days. 30 wt.% BaCO₃ by solid replacement was added to these systems. Hydration was stopped at specific times by quenching the samples in acetone for 3 days followed by drying under vacuum. Microstructure and phases formed were studied using scanning electron microscopy (SEM/EDX), X-ray diffraction (XRD) and early hydration (up to 72 h) using isothermal conduction calorimetry (ICC).

Laboratory synthesised C₃A, CaSO₄·2H₂O and BaCO₃ were mixed by hand with a molar ratio of 1:1:1 in an excess of distilled water (approximately 10:1 w/s) to form a slurry under a nitrogen blanket, to minimise carbonation. The slurry was mixed continuously for up to 24 h. A sample was taken at 2 and 24 h, and then vacuum filtered, washed and dried over silica gel, for analysis of the precipitates.

Powdered samples (passing 63 μm) for XRD were scanned either between 5 and 65° 2θ at 2° 2θ/min, or between 5 and 25° 2θ at 0.5° 2θ/min, using a Siemens D500 diffractometer with CuKα radiation set at 30 kV/40 mA. SEM(EDX) was performed at the Laboratory of Construction Materials at the Ecole Polytechnique Fédérale de Lausanne (EPFL) using a FEI quanta 200 ESEM, with a SiLi EDS detector from PGT. Samples were prepared by mounting in a cold set resin and polished to ¼ μm in a diamond spray and carbon coated. Quantitative analyses were performed using external standard mineral calibration. All micrographs presented were taken using the backscattered electron imaging (BSEI) mode.

Isothermal conduction calorimetry (ICC) was performed at 25 °C, 40 °C and 60 °C using a Wexham Developments JAF Calorimeter. 15 g of powder was mixed with the required volume of distilled water and placed in a sealed plastic bag in the ICC cells, and the rate of heat evolution measured for up to 72 h.

3. Results

3.1. Phase analysis

3.1.1. OPC with BaCO₃

On addition of BaCO₃ to OPC, the hydration products identified at 20 °C were calcium hydroxide, ettringite and calcium monocarboaluminate (Mc) (Fig. 1). CaCO₃ may form, however was not identified using XRD. This may be a consequence of overlapping peaks from BaCO₃ and BaSO₄. BaSO₄ was formed from a reaction between BaCO₃ and SO₄^{2−} ions from

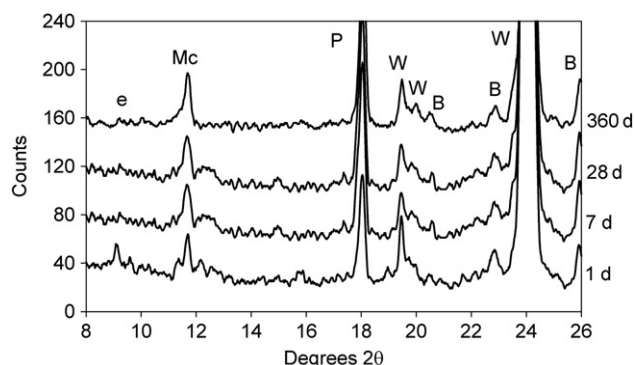


Fig. 1. OPC with 30 wt.% BaCO₃ w/s 0.37 cured at 20 °C between 24 h and 360 days. Mc – calcium monocarboaluminate, P – Ca(OH)₂, W – BaCO₃, B – BaSO₄, and e – ettringite.

the hydrating OPC. A large amount of BaCO₃ did not react. Ettringite was observed after curing at 24 h alongside calcium monocarboaluminate, but after 7 days peaks were significantly weaker. The calcium monocarboaluminate phase persisted, in this case, up to 360 days.

Curing at 60 °C gave similar results and a comparison between XRD at 20 and 60 °C after 360 days is shown in Fig. 2. At 60 °C BaSO₄ was again observed, but Mc was not. Weak peaks for a hydrogarnet-type phase were identified. Hydrogarnet formation is considered to be kinetically inhibited, and hence is more often observed at higher curing temperatures. While the presence of BaSO₄ suggests that decomposition of BaCO₃ has occurred, calcite, the most likely phase to form in the absence of Mc, could not be positively identified using XRD. But in view of the level of portlandite present this is likely to be the sink for the released CO₃²⁻ ions. Aluminate from the decomposition of Mc may be incorporated into the hydrogarnet phase.

3.1.2. 9:1 BFS:OPC with BaCO₃

The hydration products formed from the reaction between BaCO₃ and 9:1 BFS:OPC are shown in Fig. 3. Again calcium monocarboaluminate (Mc) and weak BaSO₄ peaks were observed, but they were smaller than for the neat OPC system as there is less sulfate available. Ettringite and portlandite peaks were not observed, however, this is not unusual in a high replacement level BFS composite cement [23]. Initially, after 1 day hydration, Mc was not detected, but after 7 days, sufficient reaction had occurred for Mc to form. At this point, weak peaks for BaSO₄ were detected. As in previous samples calcite was not identified.

Fig. 4 shows a comparison between a 9:1 BFS:OPC sample with 30 wt.% BaCO₃ cured at 20 and 60 °C. In contrast to that shown in Fig. 2, Mc is stable at both temperatures. At 20 °C the peak assigned to Mc is highly asymmetric but at 60 °C has split into a doublet, suggesting the presence of a hydrotalcite-type phase often found in BFS/OPC composite cements [10,23]. Hydrotalcite is a Mg–Al layered

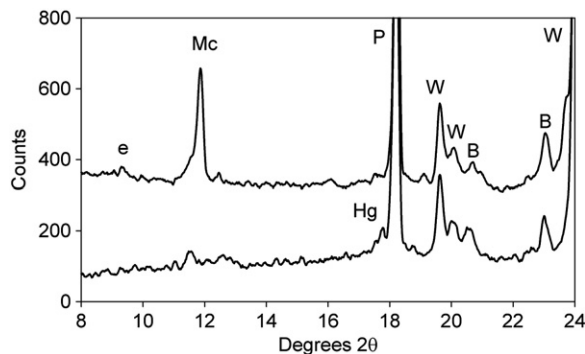


Fig. 2. OPC with 30 wt.% BaCO₃ w/s 0.37 cured at 20 and 60 °C for 360 days. Mc – calcium monocarboaluminate, P – Ca(OH)₂, W – BaCO₃, B – BaSO₄, e – ettringite, and Hg – hydrogarnet-type phase.

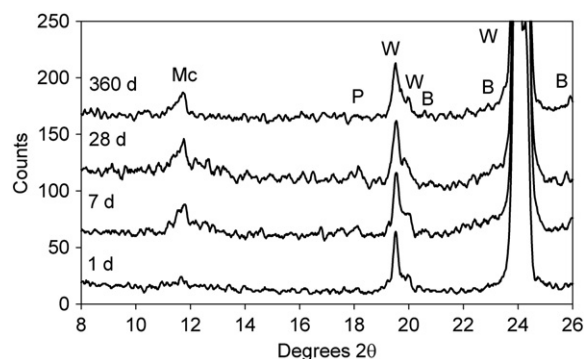


Fig. 3. 9:1 BFS:OPC 30 wt.% BaCO₃ cured at 20 °C between 24 h and 360 days. Mc – calcium monocarboaluminate, W – BaCO₃, and B – BaSO₄.

double hydroxide similar to the natural mineral Mg₆Al₂(OH)₁₆CO₃·4H₂O [24]. Hydrotalcite-type phases may contain carbonate ions. Equally non-carbonate containing hydrotalcite may be formed. It is difficult to distinguish between carbonate and non-carbonate containing hydrotalcite from qualitative XRD, and therefore substitution of CO₃²⁻ into this phase cannot be concluded. Hydrotalcite is however more stable than Mc, particularly at higher temperatures, so retention of ¹⁴C carbonate in this phase would be more desirable.

At 60 °C the hydration of the BFS is accelerated, providing sufficient quantities of aluminium and magnesium ions, which encourage hydrotalcite to form. This reaction also proceeds at 20 °C, but at a slower rate and the product is not as crystalline. Curing at 60 °C also causes hydrogarnet to form, although there is still some Mc present. The stability of Mc at 60 °C in the BFS:OPC system may be due to increased [Al³⁺] although with Mg²⁺ present it usually reacts to form the hydrotalcite. The stability of Mc is not well defined and is influenced by pH, [Al³⁺], temperature, etc.

3.1.3. C₃A, BaCO₃ and CaSO₄·2H₂O

The reaction between C₃A, BaCO₃ and CaSO₄·2H₂O was studied as a simplified reaction between components, in particular to analyse the initial formation of hydration products, such as ettringite in the presence of BaCO₃. Fig. 5 shows XRD of the system after 2 and 24 h of hydration in an excess of distilled-decarbonated water.

After reacting for 2 h, C₃A peaks were not observed. Strong BaCO₃ peaks were detected along with weaker gypsum peaks. Both ettringite and BaSO₄ formed showing that although BaSO₄ is the most insoluble species in this system, other sulphate containing phases initially form. Mc was not observed.

After 24 h of reaction, the intensity of the BaCO₃ peaks had decreased significantly, while the intensity of the BaSO₄ peaks had increased. Ettringite was also still observed, however, the intensity of its peaks had decreased, suggesting the phase was decomposing. Due to the reaction

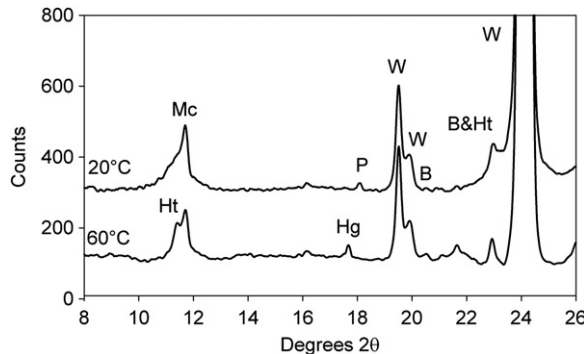


Fig. 4. 9:1 BFS:OPC 30 wt.% BaCO₃ cured at 20 °C and 60 °C for 360 days. Mc – calcium monocarboaluminate, W – BaCO₃, B – BaSO₄, P – Ca(OH)₂, Ht – hydrotalcite, and Hg – hydrogarnet.

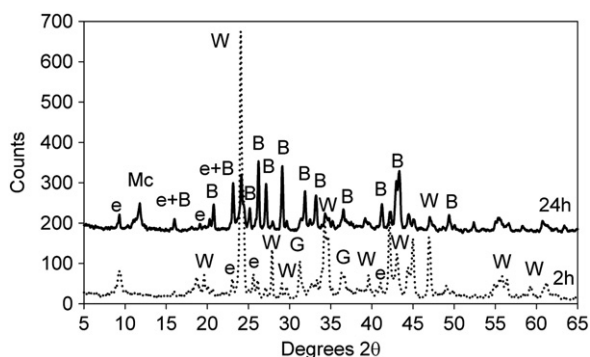


Fig. 5. 1:1:1 $C_3A:BaCO_3:CaSO_4 \cdot 2H_2O$ cured at room temperature for 2 h and 24 h. Mc – calcium monocarboaluminate, P – $Ca(OH)_2$, W – $BaCO_3$, B – $BaSO_4$, G – gypsum, and e – ettringite.

of $BaCO_3$ with gypsum to form $BaSO_4$, sufficient carbonate was released into the solution to form Mc, suggesting that the formation of $BaSO_4$ drives the release of carbonate ions into the solution and the formation of Mc.

3.2. Microstructural analysis

3.2.1. OPC with $BaCO_3$

Backscattered electron images (BSEI) of polished cement samples were taken to examine the microstructure. Fig. 6 shows an OPC clinker particle with a hydration rim within a matrix of $BaCO_3$ particles and other outer hydration products after 720 days hydration at 20 °C. The particles containing barium (e.g. $BaCO_3$ or $BaSO_4$) are the brightest spots observed in the image, due to the high atomic number of barium (197) compared to other elements present. EDX analysis of the C–S–H gel formed around the hydrating particle suggests the presence of trace amounts of barium within the C–S–H gel but this barium rich zone of C–S–H gel has a low sulfur content, indicating that the barium is not present within this region as $BaSO_4$. No EDX evidence was found either to suggest the substitution of barium into Mc or other Aft/AFm phases, as reported by Dumitri et al. [13,14]. Fig. 7 shows a comparable feature in a sample cured at 60 °C, where there is little anhydrous material present with the exception of C_4AF which was visibly hydrating, indicating hydration has been accelerated at 60 °C. In contrast to the sample cured at 20 °C, barium was not detected to any significant level within the C–S–H gel in the hydration rim analysed suggesting that whereas barium is incorporated into C–S–H at 20 °C, at 60 °C this does not occur. The hydration products formed at elevated temperatures are typically denser than those formed at

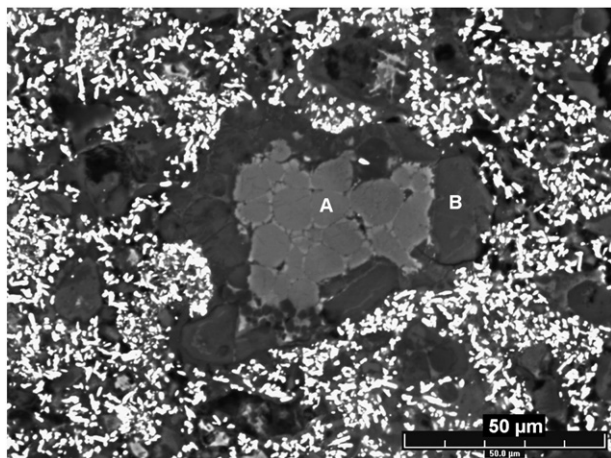


Fig. 6. OPC with 30 wt.% $BaCO_3$ cured for 720 days at 20 °C, A – anhydrous OPC, and B – hydration rim containing traces of barium.

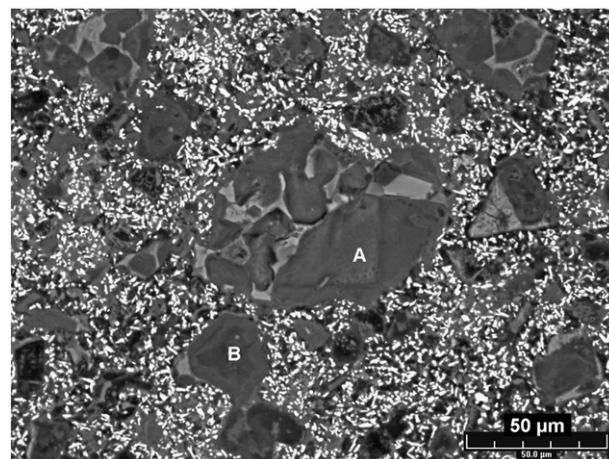


Fig. 7. OPC with 30 wt.% $BaCO_3$ cured for 720 days at 60 °C. A – Completely reacted particle, which shows no traces of barium, and B – completely reacted particle showing paler rim.

ambient temperatures [25], so diffusion of the large barium ions into the structure may not be permitted. Consideration was given to the fact that the barium signal may originate from $BaCO_3$ particles below the plane of the image, but given the difference observed between the 20 °C and 60 °C samples, it suggests the result is real.

Another unique feature in the $BaCO_3$ doped OPC samples is the presence of voids, as shown in Fig. 8. Both the shape of the voids and the presence of hydration rims indicate that the origin of the majority

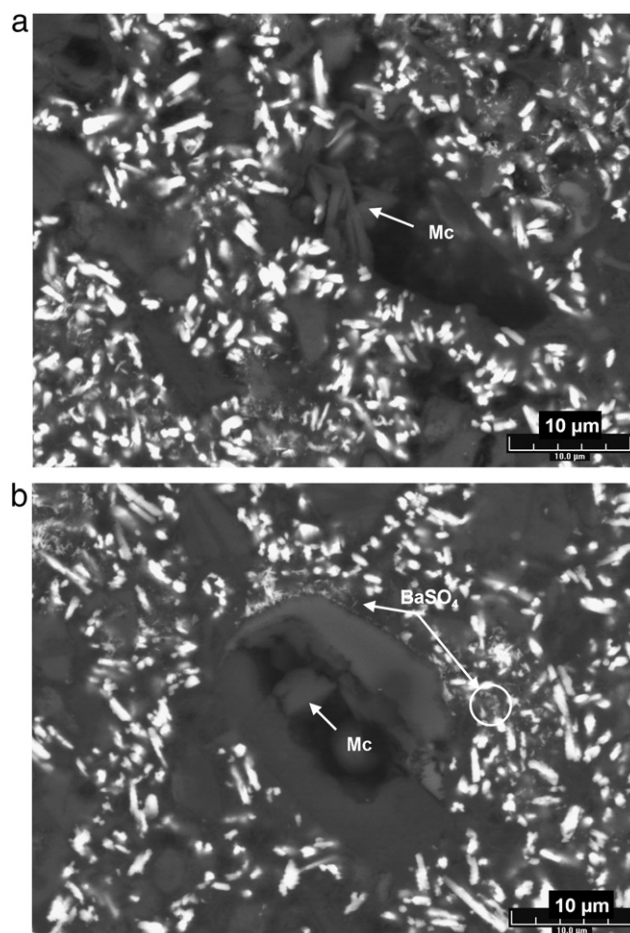


Fig. 8. a and b: OPC with 30 wt.% $BaCO_3$ cured for 720 days at 20 °C showing voids containing precipitated hydration product identified as Mc using EDX and fine particulates of $BaSO_4$.

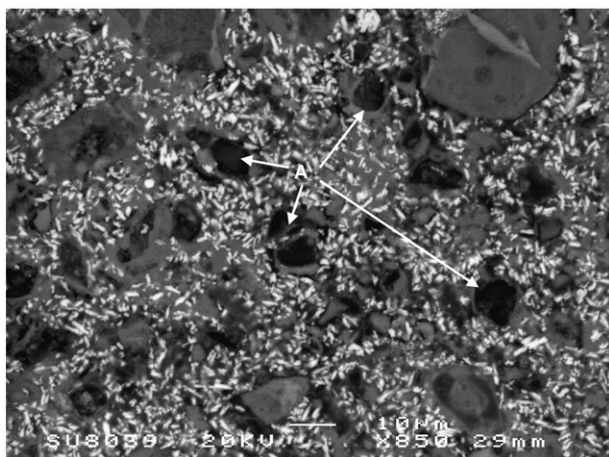


Fig. 9. OPC with BaCO₃ cured for 90 days at 60 °C showing empty voids (A).

of these hollow shells is the complete hydration of OPC particles, driven by the high relative water to cement ratio and the presence of many fine particulates. Platelet-like hydration products were observed within the voids, and identified by EDX as Mc. Fig. 8a and b shows typical shells observed in the microstructure and within them small platelet-like crystals. Similar voids have also been observed in OPC systems hydrated with large amounts of silica fume (up to 50%), with AFm phases precipitated in these hollow shells after 90 days of hydration [26] mirroring the precipitation of Mc in voids in this study. Fine BaSO₄ particles were also identified by EDX, dispersed throughout the microstructure, as indicated in Fig. 8b.

At 60 °C the voids were also observed (Fig. 9), however, a significant number were empty, corroborating the XRD results, which suggests that Mc is unstable in this system at 60 °C.

3.2.2. 9:1 BFS:OPC containing BaCO₃

In the 9:1 BFS:OPC system, BaCO₃ dominates the microstructure, as shown in Fig. 10. Anhydrous OPC was not observed, and the larger BFS particles appeared not to have reacted significantly. The voids observed in neat OPC samples were not present, so any Mc formed may be assumed to be dispersed throughout the microstructure. The samples cured at 60 °C showed few microstructural differences, aside from thin hydration rims surrounding some of the larger BFS particles, which follows with the greater amount of hydrotalcite observed at 60 °C.

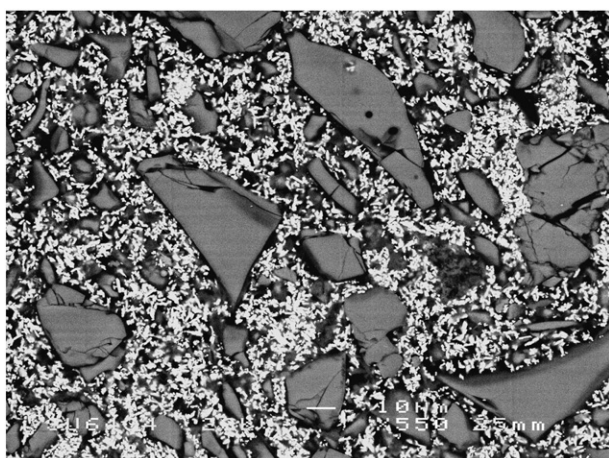


Fig. 10. 9:1 BFS:OPC 30 wt.% BaCO₃ 20 °C 720 days.

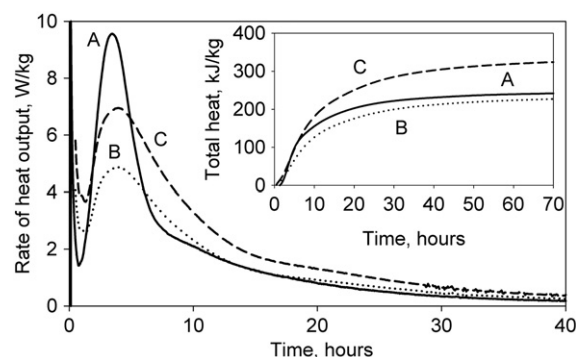


Fig. 11. Rate and total heat output for A – neat OPC, B – OPC with 30 wt.% BaCO₃, and C – normalised OPC with 30 wt.% BaCO₃ cured at 40 °C.

3.2.3. Isothermal conduction calorimetry

3.2.3.1. Addition of BaCO₃. The addition of BaCO₃ to OPC, 9:1 BFS:OPC and BFS systems has a significant effect on the heat of hydration. Fig. 11 shows the heat output of OPC both with and without BaCO₃ hydrated at 40 °C. ICC was also performed at 20 and 60 °C, presented later, on OPC and 9:1 BFS:OPC with BaCO₃ systems.

On the addition of BaCO₃, the maximum rate of heat output, q_{\max} , decreased from 9.6 Wkg⁻¹ to 4.5 Wkg⁻¹, whereas t_{\max} , the time at which q_{\max} occurs, was similar for both samples. The integral of the rate curve gives the total heat output overtime, Q . After 72 h, the normalised Q_{72} was similar for both doped and undoped samples. Normalising the curves to take into account the dilution effect of replacing 30 wt.% of OPC with BaCO₃, showed that the maximum rate of heat output (6.5 Wkg⁻¹) was still less than for neat OPC. The normalised total heat output curves, in contrast, showed a greater value for the doped system after 72 h, than for neat OPC, suggesting BaCO₃ is reacting and not acting as a dilutant alone.

Fig. 12 shows data for 9:1 BFS:OPC system, neat and with 30 wt.% BaCO₃ hydrated at 40 °C. Typically in neat 9:1 BFS:OPC, two peaks are observed, Peak II (attributed to the hydration of OPC) and Peak S (attributed to the hydration of the slag) [25]. These features can be clearly observed for neat 9:1 BFS:OPC in Fig. 12. However with 9:1 BFS:OPC containing BaCO₃, Peak II was completely suppressed and Peak S for both doped and undoped samples had similar t_{\max} and q_{\max} (1.2 Wkg⁻¹). When the data was normalised, the total heat output curve was greater after 72 h than for the neat 9:1 BFS:OPC sample.

To observe the effect of BaCO₃ on BFS alone, ICC was performed on a BFS system containing 30 wt.% BaCO₃. The tests were performed at 40 °C instead of at room temperature, due to the high signal to noise ratio at 25 °C. To assess the effect of the water to BFS ratio, as a

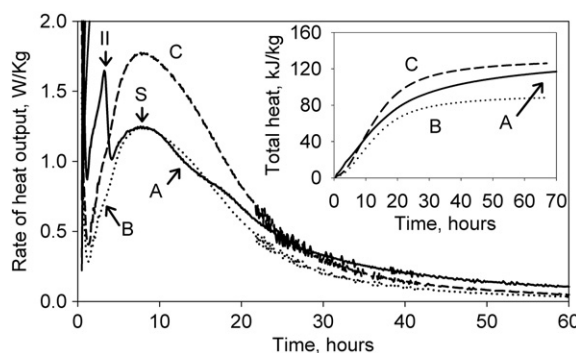


Fig. 12. Rate and total heat output for A – neat 9:1 BFS:OPC, B – 9:1 BFS:OPC with 30 wt.% BaCO₃, and C – normalised 9:1 BFS:OPC with 30 wt.% BaCO₃ cured at 40 °C.

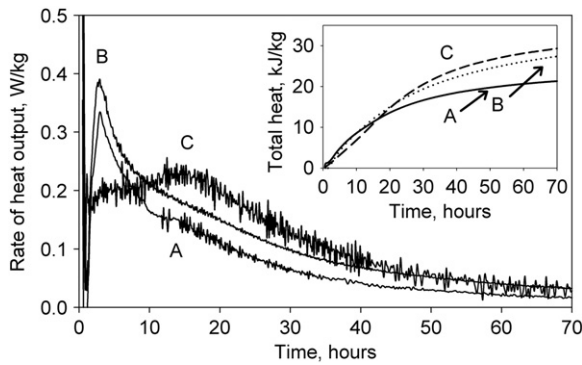


Fig. 13. Rate and total heat output for BFS with and without BaCO₃ cured at 40 °C. A – BFS w/s 0.35, B – BFS w/s 0.5, and C – BFS 30 wt.% BaCO₃ w/s 0.35.

consequence of adding BaCO₃, a neat BFS system was tested at a high (0.5) and low (0.35) water to solid ratio at 40 °C. The results (Fig. 13) have a high signal to noise ratio because of the low slag reactivity and small heat outputs measured. Only one small peak was observed for the 100% BFS samples, attributed to activation and hydration of the BFS. When the water to solid ratio was increased, q_{\max} increased slightly.

In contrast, two peaks were observed for the BaCO₃ containing sample and a greater total heat of hydration curve obtained. Normalised, the total heat evolved was approximately 100% greater for the BFS/BaCO₃ sample, implying that the BaCO₃ activates the BFS. This could be due to a combination of factors. The pH of the BaCO₃ slurry was measured and shown to be slightly alkaline, which may aid in activating the BFS. The higher water to cementitious solid ratio, the presence of fine BaCO₃ particles providing nucleation sites and also the extraction of sulfur species from the slag and precipitation of BaSO₄, may also contribute.

3.2.3.2. Increase in temperature. Fig. 14 shows the rate of heat output in kW/kg and total heat output in kJ/kg over time for OPC containing 30 wt.% BaCO₃ cured at 25 °C, 40 °C and 60 °C for the first 72 h of hydration. Increasing the temperature from 25 °C to 60 °C, increased q_{\max} from 1.7 W/kg to 11.1 W/Kg, whereas t_{\max} , decreased from 10.3 to 3.7 h. This shows that hydration is accelerated with increasing temperature [25]. The shape of the curve at 25 °C differed to the curves of the samples at 40 °C and 60 °C. The total heat outputs for 40 and 60 °C samples were similar, flattening off to approximately the same total heat output of 225 kJ/kg after 50 h suggesting that the presence of BaCO₃ is offset by the increase in temperature. At 25 °C the heat output was significantly retarded between 0 and 10 h, which is likely due to dilution.

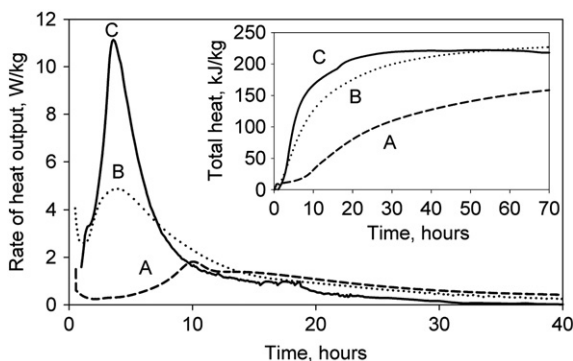


Fig. 14. Rate of heat output and total heat output for OPC with 30 wt.% BaCO₃ hydrated at 25, 40 and 60 °C w/s 0.37. A – 20 °C, B – 40 °C, and C – 60 °C.

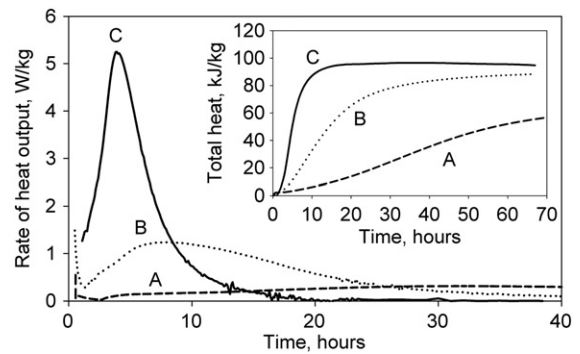


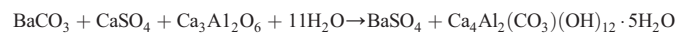
Fig. 15. Rate of heat output and total heat output for 9:1 BFS:OPC with 30 wt.% BaCO₃ hydrated at 25, 40 and 60 °C w/s 0.37. A – 20 °C, B – 40 °C, and C – 60 °C.

Fig. 15 shows the rate of heat output and total heat for 9:1 BFS:OPC with 30 wt.% BaCO₃ with increasing temperature from 25 °C to 60 °C. Increasing the temperature from 25 °C to 60 °C, increased q_{\max} from 0.31 to 5.2 W/kg, and decreased t_{\max} significantly from approximately 32 h to 4 h, indicating that the hydration of BFS is strongly thermally activated [25]. As with the OPC/BaCO₃ samples, at 25 °C the total heat output was significantly lower than for the samples cured at 40 °C and 60 °C.

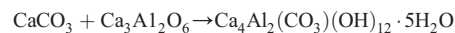
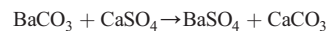
4. Discussion

4.1. Interaction of BaCO₃ with OPC

In an undoped OPC system, C₃A reacts with any soluble sulfate species to form ettringite within the first 24 h. In a doped system, BaCO₃ interferes in this process through a reaction between BaCO₃ and soluble sulfate to form BaSO₄. Despite the very low solubility of BaCO₃ (Table 1), sufficient Ba²⁺ ions enter the solution so that the solubility product of BaSO₄ is exceeded. In an OPC sample containing 30 wt.% BaCO₃, there is approximately 9 times the amount of Ba²⁺ ions present to completely react with all available SO₄²⁻. On formation of BaSO₄, carbonate is released. XRD showed this to react with aluminates to form calcium monocarboaluminate phase, Ca₄Al₂(CO₃)(OH)₁₂·5H₂O (Mc). CaCO₃ was not identified, however may form as an intermediate phase e.g.

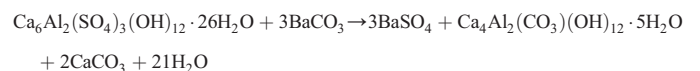


or



While hemicarboaluminate, (Ca₄Al₂(CO₃)_{0.5}(OH)₁₃·5.5H₂O), has been reported to form first in an OPC/CaCO₃ system, followed by the slow formation of Mc [7,16], no trace of hemicarboaluminate was detected using XRD in the OPC/BaCO₃ system. Hemicarboaluminate is unstable at high carbonate activities [9]. The excess of carbonate in this system appears to be sufficient to suppress its formation.

Although BaSO₄ is the most insoluble sulfate containing phase in this system, ettringite was initially observed by XRD. The two reactions, ettringite formation and BaSO₄ precipitation, therefore occur simultaneously, competing for the sulfate ions in the solution. While ettringite is initially present, XRD suggests that it decomposes to form Mc and BaSO₄, for example by the reaction below, where CaCO₃ may be formed.



The presence of large quantities of BaCO₃ maintains a sufficiently high concentration of Ba²⁺ ions in the solution to ensure all sulfate

eventually precipitates as BaSO_4 . The decomposition of ettringite is likely to occur after all calcium sulfate has been consumed in forming BaSO_4 .

ICC showed the hydration of OPC, 9:1 BFS:OPC and BFS were altered by the presence of BaCO_3 . Normalised q_{max} was lower for OPC with BaCO_3 than for the neat OPC sample. Typically, when small additions of CaCO_3 are added to OPC, the rate of hydration, q_{max} , increases due to the accelerated dissolution of C_3S and precipitation of $\text{Ca}(\text{OH})_2$, which contrasts with the decrease in q_{max} observed in this study. Other authors have reported the inhibition of OPC hydration with BaCO_3 additions, due to the formation and presence of insoluble compounds [20,21].

In contrast, the normalised Q_{72} for OPC containing BaCO_3 was greater than Q_{72} for neat OPC. This indicates that BaCO_3 is not just acting as a dilutant. A higher Q_{72} could suggest greater hydration. However additional reactions occur in the BaCO_3 containing samples (e.g. see previous equations) which may contribute to the total heat recorded. Experiments showed that additional aluminate reactions occur between 2 and 24 h. The presence of fine particulates can also accelerate hydration of cement by providing nucleation sites for hydration products to form [18,19]. This and a higher effective water to cement ratio may also contribute to the greater Q_{72} observed.

The primary difference between the reaction of CaCO_3 and BaCO_3 in cements is due to the difference in solubility of the corresponding sulfate phases. At 20–25 °C BaCO_3 is more soluble than BaSO_4 , whereas the opposite is true for the calcium compounds. Any Ca^{2+} ions released may therefore contribute to the hydration reactions, forming hydration products. In contrast, Ba^{2+} released into the solution reacts preferentially with sulfate ions producing an even more insoluble phase than BaCO_3 , which may inhibit further reactions.

4.2. Interaction of BaCO_3 with BFS

In a 9:1 BFS:OPC system with added BaCO_3 , similar phases were formed (Mc, BaSO_4), however to a lesser extent due to the lower sulfate content, as a consequence of reduced OPC content, which reacts most significantly with BaCO_3 . The additional phase, hydrotalcite was positively identified, and was encouraged to form with increasing hydration temperature.

ICC suggests that BaCO_3 has a positive effect on the hydration of BFS, increasing its rate of hydration over a period of days. The activation of BFS by BaCO_3 in the presence of OPC is thought to be similar to the mechanism observed for supersulfated cements, where setting and hardening are associated with the formation of Aft/AFm phases from ions released from BFS, OPC and calcium sulfate [10]. In a similar manner, the release of CO_3^{2-} from BaCO_3 as BaSO_4 forms allows the formation of Mc, with constituents released from the slag and hydrating OPC, albeit forming fewer hydration products. BaCO_3 in the solution is mildly alkaline. This and the fine particulates of BaCO_3 , which act as nucleation and growth sites, accelerate the dissolution of the slag. The formation of phases, such as hydrotalcite, which may also contain carbonate ions, may be encouraged to form by the excess of carbonate ions in the solution.

4.3. Encapsulation of ^{14}C

Although ^{14}C may be released by the reaction of BaCO_3 with soluble sulfate, Mc forms, thereby removing ^{14}C from the pore solution reducing its mobility. The stability of Mc formed in both cement systems was good at ambient temperatures, under high humidity conditions. However, in the OPC matrix the phase was thermally unstable and decomposed after prolonged hydration at 60 °C. A similar decomposition temperature was reported by Fentiman [27] for Mc formed in calcium aluminate cements reacted with CaCO_3 . It is suggested that Mc decomposes at 60 °C in OPC to form hydrogarnet, and the CO_3^{2-} forms CaCO_3 . In contrast, in the 9:1

BFS:OPC system, the phase was stable at 60 °C along with the hydrotalcite formed, possibly due to the higher $[\text{Al}^{3+}]$.

While Mc is observed in OPC/ CaCO_3 systems it is not stable in sulfate or chloride containing environments, where it forms ettringite and chloroaluminate respectively. An OPC/ BaCO_3 system is less likely to be susceptible to sulfate attack, because of the presence of an excess of BaCO_3 , which can react with sulfate forming BaSO_4 instead of ettringite, meaning the Mc phase is likely to persist, containing any ^{14}C .

5. Conclusion

- BaCO_3 reacts significantly with OPC, scavenging all available SO_4^{2-} ions forming BaSO_4 with the released CO_3^{2-} ions forming mono-carboaluminate. The reactivity of the BaCO_3 waste is determined by the sulfate content in the cement system.
- When a 9:1 BFS:OPC system is used to encapsulate BaCO_3 , this reaction is minimised due to lower CaSO_4 content, and hydrotalcite is formed, which may also accommodate $^{14}\text{CO}_3^{2-}$.
- Although small amounts of monocarboaluminate and hydrotalcite form, the predominant carbonate phase is, and is likely to remain, BaCO_3 .
- The presence of BaCO_3 enhances the hydration of the BFS. Mc is stabilised at 60 °C in the BFS system. Therefore, the ^{14}C in BaCO_3 may be effectively encapsulated in high replacement level BFS composites.

Acknowledgements

The authors wish to thank the EPSRC (CASE award grant number 02300221), the National Nuclear Laboratory (NNL) and the Pottery Mechanics Institute (PMI) Trust for funding.

References

- [1] M.-S. Yim, F. Caron, Life cycle and management of carbon-14 from nuclear power generation, *Progr. Nucl. Energy* 48 (2006) 2–36.
- [2] J.D. Palmer, G.A. Fairhall, Properties of cement systems containing intermediate level wastes, *Cem. Concr. Res.* 22 (2–3) (1992) 325–330.
- [3] V.L. Bonavetti, V.F. Rahhal, E.F. Irassar, Studies on carboaluminate formation in limestone filler-blended cements, *Cem. Concr. Res.* 31 (6) (2001) 853–859.
- [4] S. Tsvili, G. Batis, E. Chaniotakis, Gr. Grigoriadis, D. Theodossis, Properties and behaviour of limestone cement, concrete and mortar, *Cem. Concr. Res.* 30 (10) (2000) 1679–1683.
- [5] N. Voglis, G. Kakali, E. Chaniotakis, S. Tsvili, Portland-limestone cements. Their properties and hydration compared to those of other composite cements, *Cem. Concr. Compos.* 27 (2) (2005) 191–196.
- [6] T. Matschei, B. Lothenbach, F.P. Glasser, The role of calcium carbonate in cement hydration, *Cem. Concr. Res.* 37 (4) (2007) 551–558.
- [7] B. Lothenbach, G. Je Saout, E. Gallucci, K. Scrivener, The influence of limestone on the hydration of Portland cements, *Cem. Concr. Res.* 38 (6) (2008) 848–860.
- [8] T. Schmidt, B. Lothenbach, M. Romera, J. Neuenschwander, K. Scrivener, Physical and microstructural aspects of sulfate attack on ordinary and limestone blended Portland cements, *Cem. Concr. Res.* 39 (12) (2009) 1111–1121.
- [9] T. Matschei, F.P. Glasser, Temperature dependence, 0 to 40 °C, of the mineralogy of Portland cement paste in the presence of calcium carbonate, *Cem. Concr. Res.* 40 (2010) 763–777.
- [10] H.F.W. Taylor, *Cement Chemistry*, 2nd Ed. Thomas Telford Publishing, London, 1997.
- [11] P.C. Hewlett, *Lea's Chemistry of Cement and Concrete*, 4th Ed. Butterworth-Heinemann, London, 2001.
- [12] J. Bensted, S. Prakash Varma, Investigations of strontium and barium substitution in ettringite, *Cem. Technol.* 3 (5) (1972) 185–187.
- [13] G. Dumitru, T. Vázquez, F. Puertas, M.T. Blanco-Varela, Influencia de la adición del BaCO_3 sobre la hidratación del cemento Portland, *Mater. Constr.* 49 (254) (1999) 43–48.
- [14] G. Dumitru, T. Vázquez, F. Puertas, M.T. Blanco-Varela, Influence of BaCO_3 on the hydration of C_3A , *Proc. 10th Internat. Symp. Chem. Cem., Gothenburg*, 3, 1997, pp. 5–9.
- [15] CRC Handbook of Chemistry and Physics – 2005–2006, in: David R. Lide (Ed.), 86th ed, Taylor and Francis Group, USA, 2005.
- [16] H.J. Kuzel, H. Poellmann, Hydration of C_3A in the presence of $\text{Ca}(\text{OH})_2$, $\text{CaSO}_4 \cdot 2\text{H}_2\text{O}$ and CaCO_3 , *Cem. Concr. Res.* 21 (1991) 885–895.
- [17] M.A. Trezza, A.E. Lavat, Analysis of the system $3\text{CaO} \cdot \text{Al}_2\text{O}_3 - \text{CaSO}_4 \cdot 2\text{H}_2\text{O} - \text{CaCO}_3 - \text{H}_2\text{O}$ by FT-IR spectroscopy, *Cem. Concr. Res.* 31 (6) (2000) 862–872.
- [18] V.S. Ramachandran, Thermal analysis of cement components hydrated in the presence of calcium carbonate, *Thermochim. Acta* 127 (1988) 385–394.

- [19] V.S. Ramachandran, Cement with calcium carbonate additions, *Proceedings of the 8th Internat. Congr. Chem Cem.*, Rio de Janeiro, 5, 1986, pp. 178–182.
- [20] H.G. McWhinney, M.W. Rowe, D.L. Cocke, J.D. Ortego, Gu-Sheng Yu, X-ray photoelectron and FTIR spectroscopy investigation of cement doped with barium nitrate, *J. Environ. Sci. Health A25* (5) (1990) 463–477.
- [21] S.K. Ouki, C.D. Hills, Microstructure of Portland cement pastes containing metal nitrate salts, *Waste Manage.* 22 (2) (2002) 147–151.
- [22] G. Mendéndez, V. Bonavetti, E.F. Irassar, Strength development of ternary blended cement with limestone filler and blast-furnace slag, *Cem. Concr. Compos.* 25 (1) (2003) 61–67.
- [23] I.G. Richardson, C.R. Wilding, M.J. Dickson, The hydration of blast furnace slag cements, *Adv. Cem. Res.* 2 (8) (1989) 147–157.
- [24] M.C. Gastuche, G. Brown, M.M. Mortland, Mixed magnesium–aluminium hydroxides I. Preparation and characterisation of compounds formed in dialysed systems, *Clay Miner.* 7 (1967) 177–192.
- [25] J.I. Escalante-Garcia, J.H. Sharp, The effect of temperature on the early hydration of Portland cement and blended cements, *Adv. Cem. Res.* 12 (3) (2000) 121–130.
- [26] K.O. Kjellsen, B. Lagerblad, H.M. Jennings, Hollow-shell formation – an important mode in the hydration of Portland cement, *J. Mat. Sci.* 32 (1997) 2921–2927.
- [27] C.H. Fentiman, Hydration of carbo-aluminous cement at different temperatures, *Cem. Concr. Res.* 15 (4) (1985) 622–630.